

Amplified spontaneous emission from opal photonic crystals engineered with structural defects†

Francesco Di Stasio,^a Luca Berti,^a Martin Burger,^b Franco Marabelli,^b Samuele Gardin,^c Tiziano Dainese,^c Raffaella Signorini,^c Renato Bozio^c and Davide Comoretto^{*a}

Received 1st June 2009, Accepted 30th September 2009

First published as an Advance Article on the web 22nd October 2009

DOI: 10.1039/b910734g

In this work, we report on the optical properties and amplified spontaneous emissions (ASE) of polystyrene opals engineered with planar structural defects containing a conjugated polymer emitter. Defects in opals give rise to allowed states inside the photonic stop band, which are probed by transmittance and reflectance spectroscopy. The emission spectrum of the polymer embedded in the defect layer is strongly modified and fingerprints of defect states located inside the stop band are recognized. Amplified spontaneous emission for these engineered photonic crystals is clearly observed.

1. Introduction

Photonic crystals (PhC) are materials that possess a regular and periodic modulation of the dielectric constant on a length scale comparable to the wavelength of visible light. Among them, artificial opals, *i.e.* a face centred cubic lattice of monodisperse microspheres, represent a useful system to investigate optical effects.^{1,2} Despite the fact that opals do not show a complete photonic band gap (PBG) but only a pseudogap (stop band), *i.e.* a gap only along one crystallographic direction, their versatility allows us to obtain interesting structures. Artificial opals are grown with a process based on the spontaneous assembly of microspheres into stable and well-defined structures.^{3–11} From the PhC point of view, the main drawback with opals is that their structure does not allow the formation of a complete PBG. Unlike PhC, inverse opals with the proper dielectric contrast allow the opening of a complete PBG.⁹

The main features of PhC depend on their structure and dielectric contrast.¹² With the opal structure—well defined (face centred cubic) with a unit cell length that depends on sphere diameter—possibilities to tune their properties are provided either by the modulation of the refractive index of the composing materials or by the use of spheres with different diameters. This latter approach, though useful for preparing opals suitable for work in selected spectral regions, is not compatible for operating photonic devices.¹³ For these reasons, the problem of optical response modulation is

approached by refractive index tuning through photoactive materials.

A different strategy to tune optical and photonic properties of PhC is represented by engineering structural defects.¹⁴ Indeed, defects act as photonic dopants and, depending on the structure, can trap the light inside the material. Point defects represent optical cavities where the light is highly localised within the structure.¹⁵ Linear defects work as waveguides in which the light is effectively confined within the structure by the photonic band gap.^{15–17} Moreover, the presence of a structural defect inside the dielectric lattice allows the testing of light localisation effects.^{14,15,18,19} Inside such localised states, the electric field associated to the electromagnetic wave is concentrated. Localisation effects, combined with a high quality factor of the cavity, can provide an optical feedback in order to achieve laser emission^{20–25} from localised states when an emitting material is embedded in the planar defect.^{26,27}

Several methods have been used to prepare defects inside opals and inverse opals photonic crystals.^{15,17,20,22,23,25,28–40} Recently, a very simple technique was used in order to obtain a planar active structural defect in an opal structure. A free standing polymeric film doped with suitable dyes a few microns thick was sandwiched between two opals.^{22,38,41,42} Even though such structures do not show any evidence of the optical fingerprint of defect states, amplified spontaneous emission (ASE) and lasing inside²² or at the low energy edge^{38,41} of the photonic stop band was observed.

In this work, we adopted the sandwich method to properly engineer opals with an emitting conjugated polymer embedded in the structural defect for possible lasing applications. As the active material, we have selected a functionalised poly(*p*-phenylenevinylene), which possesses the advantage, with respect to other materials, of showing a good emission efficiency in the solid state.

We show here optical evidence of defect states inside the PhC stop band due to the presence of a polymeric film between opals, which breaks the periodicity of the dielectric lattice.

^a Università degli Studi di Genova, Dipartimento di Chimica e Chimica Industriale, Via Dodecaneso 31, 16146 Genova, Italy.

E-mail: comoretto@chimica.unige.it; Fax: +39 010 3538733; Tel: +39 010 3538736

^b Università di Pavia, Dipartimento di Fisica “A. Volta”, Via Bassi 7, 27100 Pavia, Italy

^c Università degli Studi di Padova, Dipartimento di Scienze Chimiche, Via Marzolo 1, 35131 Padova, Italy

† This article was submitted as part of a web theme issue highlighting papers from the Italian national meeting on Raman spectroscopy and non linear effects.

Moreover, amplified spontaneous emission (ASE) from the sandwich structure was observed. In spite of the good optical quality of the photonic crystal system, photochemical degradation of the material occurs.

2. Experimental

2.1 Opal preparation

Commercial polystyrene monodisperse microsphere water suspensions of 10% in volume (Duke Scientific, diameter $a = 240$ or 260 nm; standard deviation $<5\%$; refractive index, $n_{\text{PS}} = 1.5$) were used for opal preparation. We properly diluted these suspensions with de-ionized water in order to obtain the desired sample thickness (about $3 \mu\text{m}$). Opal films were grown by using the meniscus technique¹⁰ at 45°C inside a BF53 Binder incubator. The sphere diameter was selected in order to match the stop band spectral position with the emission spectrum of the conjugated polymer emitter.

2.2 Doped planar defect preparation

Poly{[2-[2',5'-bis(2''-ethylhexyloxy)phenyl]-1,4-phenylenevinylene]-co-[2-methoxy-5-(2'-ethylhexyloxy)-1,4-phenylenevinylene]} (BEH-PPV) was purchased from Sigma-Aldrich and used as dopant emitter of the defect layer without further purification. Free-standing films of carboxy-terminated polystyrene ($M_w = 100.000$, Sigma-Aldrich) blended with the BEH-PPV (10:1 weight ratio) were drop-cast on glass substrates from solutions of different solvents. After solvent evaporation, the polymeric film was peeled off the substrate and sandwiched between opals thus creating the structural defect. With this technique, we were able to prepare large area free-standing films with variable thicknesses in the range of $0.6\text{--}5 \mu\text{m}$.

2.3 Spectroscopy

Transmittance (T), normal incidence reflectance (R) and photoluminescence (PL) spectra were measured with optical set-ups based on an optical fiber coupled Avantes 2048 compact spectrometer working in the $250\text{--}1100$ nm range. The sample was mounted on a rotating stage, allowing for T and PL measurements at different incidence or detection angles. The excitation for PL spectra was provided by an Oxixus (model 405-50-COL-PP) continuous wave laser diode with an emission at 405 nm and a power of 50 mW. A Semrock notch filter (model LP02-442RS-25) with a 450 nm cut-off wavelength was used to stop the exciting laser line. A previously described micro reflectance set-up with a spot size of $50 \mu\text{m}$ was used to investigate sample uniformity and morphology.⁴³

2.4 Amplified spontaneous emission

ASE experiments were performed on a titanium sapphire laser system. It delivered 150 fs pulses, with a maximum of 0.7 mJ per pulse energy, at ~ 800 nm and with a 1 kHz repetition rate. With a b-barium borate doubling crystal and a cut-off filter, a 400 nm wavelength beam was obtained. The intensity of the input beam was continuously varied with a half wave plate, a polarizer and a set of neutral density filters. The input was focused with a 200 mm focal length cylindrical lens

onto sample slides. The beam emitted from the sample was detected by an optical fiber connected to a micro-spectrometer (Ocean Optics). The transmitted beam was detected with a large area photodiode, whose signal is sampled by a 500 MHz oscilloscope (Tektronik TDS 520B). The spatial profile of the input beam was measured using a CCD camera (Pulnix TM-7CN) placed on the beam focus, and the pulse energies were sampled with a pyroelectric detector (Molelectron J3-05).⁴⁴

3. Results and discussion

3.1 Opals and defect film characterisation

Fig. 1a shows the typical reflectance spectra of the 260 nm opals used to build the sandwich structure. These spectra show reflectance peaks (transmission minimum) associated with the photonic stop band at about 582 nm. For the 240 nm opals, the stop band is shifted to 552 nm, according to photonic crystal scaling laws. The presence of an extended interference fringe pattern on both spectral sides of the stop band provides information on the optical quality of such opals. Interference fringes can also be used to calculate the thickness (d) of samples:

$$d = \frac{N_f}{2n_{\text{eff}}\Delta\tilde{\nu}} \quad (1)$$

once the effective refractive index (n_{eff}) of the opal is known by fitting transmittance spectra recorded at different incidence angles with the Bragg–Snell law,^{42,45,46} N_f is the number of fringes in the $\Delta\tilde{\nu}$ (cm^{-1}) spectral range.

The Bragg–Snell fitting of T spectra versus incidence angle (not shown here) provided a value of $n_{\text{eff}} = 1.4$. Then, from eqn (1), we found mean values of $d = 3.6 \mu\text{m}$ and $d = 2.9 \mu\text{m}$ for the two opals whose spectra are reported in Fig. 1a. Fig. 1b

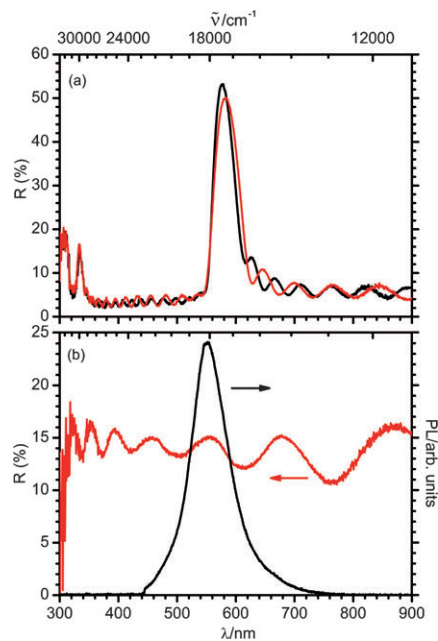


Fig. 1 (a) R spectra of opals (260 nm) used in the sandwich structure, (b) PL spectrum (black) and R spectrum (red) of the free-standing film used as doped planar defect.

shows the R spectrum for the polymer layer used to build the defect. A clear interference fringe pattern is observed. By assuming, for this film, a refraction index ($n = 1.6$) close to that of a polystyrene matrix, we found a mean thickness value of $d = 0.9 \mu\text{m}$. The PL spectrum of this film is also reported in Fig. 1b. The PL peak is at 548 nm and it shows a reasonable overlap with the photonic stop band.

3.2 Sandwich structure characterisation

After sandwiching the defect layer between opals, R and T spectra appeared strongly modified due to the presence of the film, which breaks the periodicity of the system (Fig. 2a). In particular, within the stop band, several sharp and reproducible structures are observed. A careful analysis of several tens of samples showed that such sharp structures are not due to noise. Moreover, when comparing R and T spectra (Fig. 2a) recorded at the same point of the same sample, a nice correspondence between the minima in the R spectra and the maxima in the T ones is observed. This fact indicates that an increased transparency of the photonic crystal is observed for selected frequencies within the stop band. We assign these states to defect modes induced by the periodicity break introduced by the defect layer, which modifies the density of photonic states.

The number of minima/maxima in the R/T spectra depends on the probing spot position on the sample as well as on the defect thickness. We are also aware that the presence of air gaps in our system cannot be excluded. A careful analysis of these items is in progress. We would like to point out that data reported here, as well as our preliminary findings previously published,⁴² are the first clear evidence of defect states within the stop band, which were never observed before in optical spectra for opals with structural defects prepared with the sandwich technique.^{22,38,41} We would like to stress here again

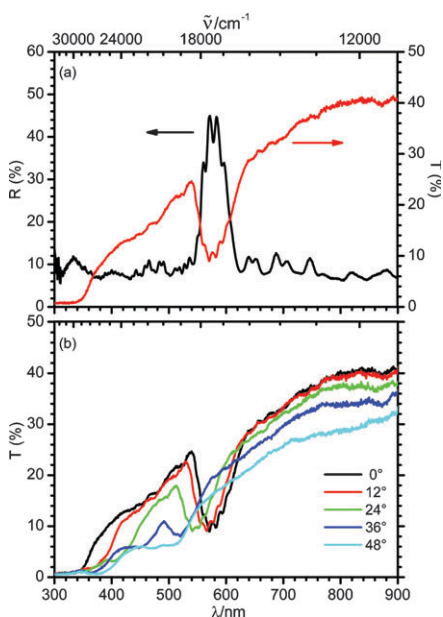


Fig. 2 (a) R (black) and T (red) spectra of opals with doped planar defect, (b) T spectra at different incidence angles.

that the number of defect states is correlated to film thickness. As a matter of fact, when planar defects in an opal are thinner than the PhC lattice parameter ($d < a\sqrt{2}$), a single minimum (maximum) is observed in the stop band spectral region of the R (T) spectrum.^{15,18,20,23,25,28,29,31,32,37} In this case, better light localization effects are expected than in our system. For $d > a\sqrt{2}$, several modes are allowed to propagate within the defect and then a corresponding number of minima (maxima) are detected in the R (T) spectra.

Fig. 2b shows the dispersion properties of defect modes in the T spectra upon changing the incidence angles. It is worth noticing that it is possible to observe defect modes for incidence angles up to 36° , indicating the high optical quality of these photonic crystals. We notice that the dispersion properties of opals with and without planar defects are similar.

After T and R characterisation of our photonic crystals, emission properties have been investigated. Fig. 3 shows the comparison of the PL spectra of the doped film before and after being inserted between opals. Once the film is enclosed between opals, the PL is strongly modified by the presence of the stop band at 582 nm that partially overlaps the PL peak (dashed area in Fig. 3). In the simplest picture, the light emitted should be filtered by the front photonic crystal, thus reducing its intensity in the stop band spectral region and, indeed, this is observed. However, in addition to such a filtering effect, the PL spectrum shows unusual emission peaks inside the spectral region forbidden to light propagation. The spectral positions of such peaks favourably match analogous features previously observed in the R and T spectra (also reported in Fig. 3 for a better comparison) and assigned to defect modes. In our opinion, the increased emission within the stop band corresponding to such peaks is a stronger demonstration of our assignment of the defect nature of the optical modes observed in R, T and PL spectra.

The dispersion properties of PL spectra for different light collection angles are reported in Fig. 4. The stop band observed in the PL spectra shows the same dispersion properties previously observed in T spectra (Fig. 2). It is noteworthy that PL modes also show a similar dispersion and defect states are observed only within the stop band for any detection angle, thus unambiguously showing their tight connection to the density of photonic states within the gap and again confirming their defect assignment.

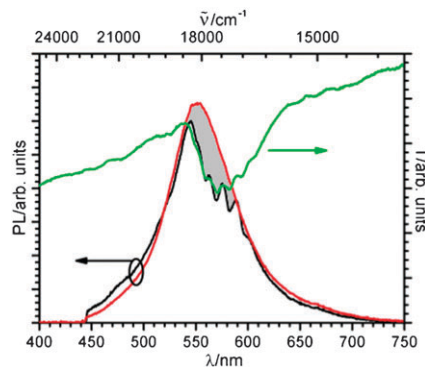


Fig. 3 PL spectra of the doped film: free standing (red); sandwiched between opals (black); T spectrum of the sandwich structure (green).

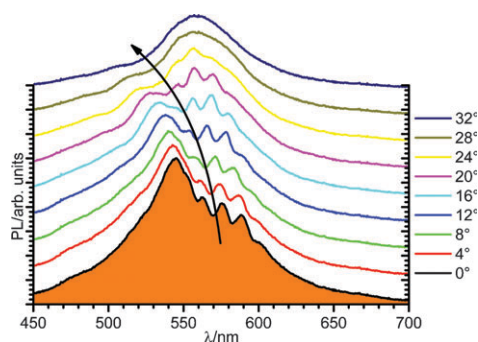


Fig. 4 PL spectra of the sandwich structure collected for different detection angles.

3.3 Amplified spontaneous emission

PL measurements *versus* excitation energies were done on samples prepared with 240 and 260 nm opals (5–6 μm thick) and planar defects of different thicknesses (2–3 μm). Fig. 5 shows the PL spectra *versus* pumping fluence for such a sample, made with 260 nm opals.

Upon increasing the excitation energy, a superlinear increase of intensity accompanied by a clear sharpening effect is observed.

This is clear evidence of an amplified spontaneous emission process. In fact, by comparing this behaviour with a free standing sample PL emission, it is evident that the sharpening effect is absent at increasing input energies (Fig. 6). Unfortunately, after a few minutes, the PL signal degrades and, at present, does not allow us to reach the lasing threshold.

Samples made with 240 nm opals show a similar behaviour. We are currently working to improve the photochemical stability of polyconjugated emitters.

4. Conclusions

Artificial polystyrene opals were grown and characterised. Free standing polystyrene films blended with BEH-PPV, a well known emitting conjugated polymer, were used to prepare opals with planar defects by the sandwich technique. A detailed optical characterisation (transmission, reflectance and photoluminescence spectroscopy) of these structures shows unambiguous evidence of well resolved defect states within the photonic stop band.

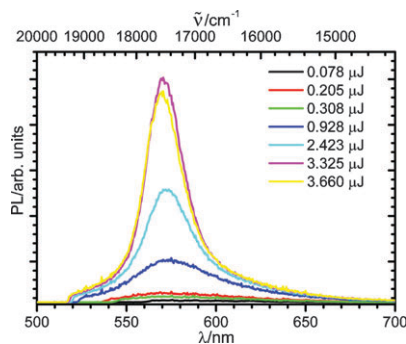


Fig. 5 PL spectra of a sandwich structure *vs.* excitation energy. Amplified spontaneous emission is observed for the highest energy values.

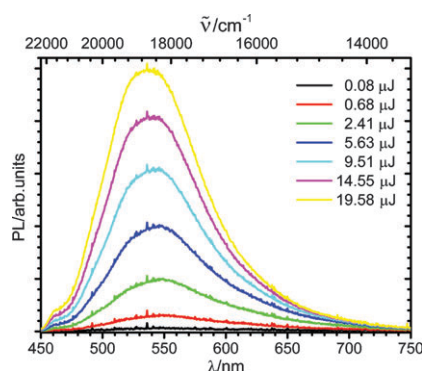


Fig. 6 PL spectra of the free standing film *vs.* excitation energy.

Amplified spontaneous emission of the sandwich structure was observed. However, the photochemical degradation of the emitting material prevents a detailed characterisation of the phenomenon. Other types of materials with better chemical stability need to be tested inside this kind of photonic structure.

Acknowledgements

We gratefully acknowledge financial support from the Italian Ministry of University and Research through program Progetti di Ricerca di Rilevante Interesse Nazionale 2006 (prot. 2006031511).

References

- 1 E. Yablonovitch, *Phys. Rev. Lett.*, 1987, **58**, 2059–2062.
- 2 S. John, *Phys. Rev. Lett.*, 1987, **58**, 2486–2489.
- 3 D. J. Norris, E. G. Arlinghaus, L. Meng, R. Heiny and L. E. Scriven, *Adv. Mater.*, 2004, **16**, 1393–1399.
- 4 Y. Xia, B. Gates and Z. Y. Li, *Adv. Mater.*, 2001, **13**, 409–413.
- 5 J. E. G. J. Wijnhoven and W. L. Vos, *Science*, 1998, **281**, 802–804.
- 6 A. A. Zakhidov, R. H. Baughman, Z. Iqbal, C. Cui, I. Khayrullin, S. O. Dantas, J. Marti and V. G. Ralchenko, *Science*, 1998, **282**, 897–901.
- 7 D. J. Norris and Y. A. Vlasov, *Adv. Mater.*, 2001, **13**, 371–376.
- 8 S. G. Romanov, T. Maka, C. M. S. Torres, M. Muller and R. Zentel, *Synth. Met.*, 2001, **124**, 131–135.
- 9 A. Blanco, E. Chomski, S. Grabtchak, M. Ibisate, S. John, S. W. Leonard, C. Lopez, F. Meseguer, H. Minguez, J. P. Mondia, G. A. Ozin, O. Toader and H. M. v. Driel, *Nature*, 2000, **405**, 437–440.
- 10 P. Jiang, J. F. Bertone, K. S. Hwang and V. L. Colvin, *Chem. Mater.*, 1999, **11**, 2132–2140.
- 11 P. Jiang, J. F. Bertone and V. L. Colvin, *Science*, 2001, **291**, 453–457.
- 12 J. D. Joannopoulos, R. D. Meade and J. N. Win, *Photonic Crystals: Molding the Flow of the Light*, Princeton University Press, Princeton, 1995.
- 13 F. Garcia-Santamaria, H. Minguez, M. Ibisate, F. Meseguer and C. Lopez, *Langmuir*, 2002, **18**, 1942.
- 14 J. S. Foresi, P. R. Villeneuve, J. Ferrera, E. R. Thoen, G. Steinmeyer, S. Fan, J. D. Joannopoulos, L. C. Kimerling, H. I. Smith and E. P. Ippen, *Nature*, 1997, **390**, 143–145.
- 15 P. V. Braun, S. A. Rinne and F. Garcia-Santamaria, *Adv. Mater.*, 2006, **18**, 2665–2678.
- 16 Y. H. Ye, T. S. Mayer, I. C. Khoo, I. B. Divliansky, N. Abrams and T. E. Mallouk, *J. Mater. Chem.*, 2002, **12**, 3637–3639.
- 17 Q. Yan, Z. Zhou, X. S. Zhao and S. J. Chua, *Adv. Mater.*, 2005, **17**, 1917.
- 18 J. F. Galisteo-López, M. Galli, L. C. Andreani, A. Mihi, R. Pozas, M. Ocaña and H. Míguez, *Appl. Phys. Lett.*, 2007, **90**, 101113.

-
- 19 D. Wang, J. Li, C. T. Chan, V. Salgueirino-Maceira, L. M. Liz-Marzan, S. Romanov and F. Caruso, *Small*, 2005, **1**, 122.
 - 20 E. Palacios-Lidon, J. F. Galisteo-Lopez, B. H. Juarez and C. Lopez, *Adv. Mater.*, 2004, **16**, 341.
 - 21 Q. Yan, Z. Zhou and X. S. Zhao, *Chem. Mater.*, 2005, **17**, 3069–3071.
 - 22 S. Furumi, H. Fudouzi, H. T. Miyazaki and Y. Sakka, *Adv. Mater.*, 2007, **19**, 2067.
 - 23 N. Tetreault, A. Mihi, H. Miguez, I. Rodriguez, G. A. Ozin, F. Meseguer and V. Kitaev, *Adv. Mater.*, 2004, **16**, 346.
 - 24 J. R. Lawrence, Y. Ying, P. Jiang and S. H. Foulger, *Adv. Mater.*, 2006, **18**, 300.
 - 25 L. Wang, Q. Yan and X. S. Zhao, *Langmuir*, 2006, **22**, 3481–3484.
 - 26 S. Noda, A. Chutian and M. Imada, *Nature*, 2000, **407**, 608–610.
 - 27 O. Painter, R. K. Lee, A. Scherer, A. Yariv, J. D. O'Brien, P. D. Dapkus and I. Kim, *Science*, 1999, **284**, 1819–1821.
 - 28 R. Pozas, A. Mihi, M. Ocana and H. Miguez, *Adv. Mater.*, 2006, **18**, 1183.
 - 29 A. Arsenault, F. Fleischhaker, G. v. Freymann, V. Kitaev, H. Miguez, A. Mihi, N. Tetreault, E. Vekris, I. Manners, S. Aitchison, D. Perovic and G. A. Ozin, *Adv. Mater.*, 2006, **18**, 2779–2785.
 - 30 Q. Yan, L. K. Teh, Q. Shao, C. C. Wong and Y. M. Chiang, *Langmuir*, 2008, **24**, 1796–1800.
 - 31 N. Tetreault, A. C. Arsenault, A. Mihi, S. Wong, V. Kitaev, I. Manners, H. Miguez and G. A. Ozin, *Adv. Mater.*, 2005, **17**, 1912.
 - 32 F. Fleischhaker, A. C. Arsenault, J. Schmidtke, R. Zentel and G. A. Ozin, *Chem. Mater.*, 2006, **18**, 5640–5642.
 - 33 N. Tetreault, H. Miguez, S. M. Yang, V. Kitaev and G. A. Ozin, *Adv. Mater.*, 2003, **15**, 1167.
 - 34 Y. Jun, C. A. Leatherdale and D. J. Norris, *Adv. Mater.*, 2005, **17**, 1908.
 - 35 F. Fleischhaker, A. C. Arsenault, V. Kitaev, F. C. Peiris, G. von Freymann, I. Manners, R. Zentel and G. A. Ozin, *J. Am. Chem. Soc.*, 2005, **127**, 9318–9319.
 - 36 Q. Yan, A. Chen, S. J. Chua and X. S. Zhao, *Adv. Mater.*, 2005, **17**, 2849.
 - 37 P. Massé, S. Reculosa, K. Clays and S. Ravaine, *Chem. Phys. Lett.*, 2006, **422**, 251–255.
 - 38 F. Jin, Y. Song, X.-Z. Dong, W.-Q. Chen and X.-M. Duan, *Appl. Phys. Lett.*, 2007, **91**, 031109.
 - 39 T. A. Taton and D. J. Norris, *Nature*, 2002, **416**, 685–686.
 - 40 W. Lee, S. A. Pruzinsky and P. V. Braun, *Adv. Mater.*, 2002, **14**, 271.
 - 41 F. Jin, C. Li, X. Dong, W. Chen and X. Duan, *Appl. Phys. Lett.*, 2006, **89**, 241101.
 - 42 F. Di Stasio, M. Cucini, L. Berti, D. Comoretto, A. Abbotto, L. Bellotto, N. Manfredi and C. Marinzi, *J. Europ. Opt. Soc.: Rapid Publ.*, 2009, **4**, 09033.
 - 43 E. Pavarini, L. C. Andreani, C. Soci, M. Galli and F. Marabelli, *Phys. Rev. B*, 2005, **72**, 045102.
 - 44 J. J. Jasieniak, I. Fortunati, S. Gardin, R. Signorini, R. Bozio, A. Martucci and P. Mulvaney, *Adv. Mater.*, 2008, **20**, 69–73.
 - 45 V. Morandi, F. Marabelli, V. Amendola, M. Meneghetti and D. Comoretto, *J. Phys. Chem. C*, 2008, **112**, 6293–6298.
 - 46 V. Morandi, F. Marabelli, V. Amendola, M. Meneghetti and D. Comoretto, *Adv. Funct. Mater.*, 2007, **17**, 2779–2786.